

# Frequency Combs with Parity-Protected Cross-Correlations and Entanglement from Dynamically Modulated Qubit Arrays

Denis Ilin<sup>1,2</sup>, Alexander V. Poshakinskiy,<sup>2</sup> Alexander N. Poddubny,<sup>3,\*</sup> and Ivan Iorsh<sup>1,†</sup>

<sup>1</sup>*Department of Physics and Technology, ITMO University, St. Petersburg, 197101, Russia*

<sup>2</sup>*Ioffe Institute, St. Petersburg 194021, Russia*

<sup>3</sup>*Rehovot 7610001, Israel*



(Received 1 March 2022; revised 22 August 2022; accepted 12 December 2022; published 9 January 2023)

We develop a general theoretical framework to dynamically engineer quantum correlations and entanglement in the frequency-comb emission from an array of superconducting qubits in a waveguide, rigorously accounting for the temporal modulation of the qubit resonance frequencies. We demonstrate that when the resonance frequencies of the two qubits are periodically modulated with a  $\pi$  phase shift, it is possible to realize simultaneous bunching and antibunching in cross-correlations as well as Bell states of the scattered photons from different sidebands. Our approach, based on the dynamical conversion between the quantum excitations with different parity symmetry, is quite universal. It can be used to control multiparticle correlations in generic dynamically modulated dissipative quantum systems.

DOI: [10.1103/PhysRevLett.130.023601](https://doi.org/10.1103/PhysRevLett.130.023601)

*Introduction.*—The ability to multiplex several signals at different frequencies and transmit them via one channel is of paramount importance for information processing. A single photon can also be in a quantum superposition of several frequency channels and act as a flying qudit—a multilevel analog of the qubit—that can be used for quantum computing [1]. In order to generate and process multiqubit entanglement, one must realize (i) single-qudit operations and (ii) two-qudit gates. It has already been proven theoretically and demonstrated experimentally that any single-qudit unitary operation can be performed by using a combination of phase shapers and a linear modulator [2]. Realization of two-qudit gates is more complicated. The schemes with ancillas and postselection based on Knill–Laflamme–Milburn (KLM) protocol were proposed [3]. However, the use of such gates is limited since they operate only with a certain (quite small) probability of success. An alternative approach is to make photons interact with a quantum object with nonlinear optical properties. As such, a two-level system (qubit) that cannot scatter two photons at once can operate as a simplest nonlinear sign (NS) gate for resonant photons [4]. Quantum emitters with two metastable ground states enable deterministic generation of single-rail encoded photonic cluster states [5,6]. In this Letter, we propose a tunable setup with several waveguide-coupled qubits that realizes dynamical control of cross-correlations for multiplexed emission, enabling generation of multiphoton entangled states. Such states are indispensable in various areas of the emerging quantum technologies including quantum communications [7,8] and quantum networks [9–11]; however, it is rather hard to generate them using probabilistic linear-optics approaches with low success rates, and they can be vulnerable to decoherence. The scheme we put forward

enables stable deterministic generation of entangled frequency-coded flying qudits.

We consider an array of qubits with the resonant frequencies harmonically modulated in time. Waveguide-coupled qubit arrays are now readily realized [12] and have a high potential for manipulation of quantum signals [13–17]. Temporal modulation can be achieved via the control optical pump beam for cold atom systems [18] or by means of modulated gate voltage for the case of semiconductor quantum dots or solid-state defects [19–22]. For the modulated superconducting qubits platform the state-of-the-art technology supports independent coherent modulation of each individual qubit [23]. We show that the qubit resonance modulation can drive the conversion between the even (bright) and odd (dark) states in the qubit arrays, enabling the symmetry-protected bichromatic bunching and antibunching between the photons from different sidebands.

More generally, in the sideband-resolved regime, when the modulation frequency is much larger than the qubit resonance broadening, the frequency conversion processes, similar to Stokes and anti-Stokes Raman scattering, give rise to the frequency comb in the scattered light spectrum with multiple sidebands separated by the modulation frequency. The correlations and entanglement of the frequency-filtered photons in the sidebands of the emission spectrum can be quite complex. In particular, it was shown that bunched bundles of several photons can be realized by filtering certain sidebands [24,25]. The advantage of our proposal is that the photon-photon correlations can be dynamically tuned, which is essential for most of the practical applications [26,34].

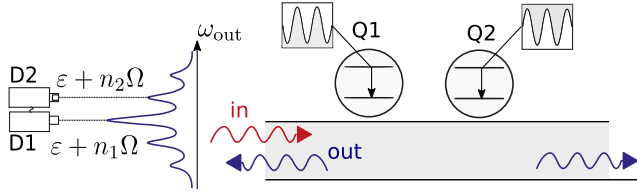


FIG. 1. Schematics of the structure under consideration. Two qubits Q1 and Q2 coupled to a waveguide are excited by coherent electromagnetic fields. Qubit resonance frequencies are modulated in time according to Eq. (1).

*Model.*—The structure under consideration consists of  $N$  superconducting qubits, coupled to the waveguide, and located at the distance  $d$ . We focus on the simplest case of  $N = 2$  qubits, shown in Fig. 1 with a generalization for  $N > 2$  discussed in Supplemental Material, Secs. (S5)–(S7) [27]. The qubit resonance frequencies  $\omega_1$  and  $\omega_2$  are modulated as

$$\omega_1(t) = \omega_0 + A \cos \Omega t, \quad \omega_2(t) = \omega_0 + A \cos(\Omega t + \alpha), \quad (1)$$

where  $\omega_0$  is the equilibrium qubit resonance frequency,  $A$  is the modulation amplitude,  $\Omega$  is the modulation frequency, and  $\alpha$  is the relative phase of the modulation. The qubits are modeled as two-level systems, characterized by the spontaneous decay rate into the waveguide  $\gamma_{1D}$ . The structure is excited from one side by a weak monochromatic coherent wave at frequency  $\varepsilon$ . We start with the sideband-resolved regime, when the modulation frequency  $\Omega$  is much larger than the qubit decay rate  $\gamma_{1D}$ , and consider resonant excitation with frequency  $\varepsilon \approx \omega_0$ . In this case, the scattered photons can have a well-defined set of frequencies that form a frequency comb,

$$\varepsilon + n\Omega, \quad n = 0, \pm 1, \pm 2, \dots, \quad (2)$$

where  $n$  is the sideband number. Our goal is to analyze the second-order cross-correlations between the scattered photons in the sidebands  $n_1$  and  $n_2$ ,

$$g_{n_1, n_2}^{(2)} = \frac{I_{n_1, n_2}^{(2)}}{I_{n_1}^{(1)} I_{n_2}^{(1)}}, \quad (3)$$

where  $I_{n_1}^{(1)}$  is the intensity of scattering of a single photon into sideband  $n_1$ , and  $I_{n_1, n_2}^{(2)}$  is the intensity of scattering of a photon pair into sidebands  $n_1$  and  $n_2$ .

*Parity-protected cross-correlations.*—From now on we consider the case when the two qubits are located at the same point, i.e.,  $\omega_0 d/c = 0$  (or  $2\pi$ ), so the system is invariant under the parity operation  $\mathcal{P}$  that interchanges the qubits. The effect of nonzero interqubit distance is analyzed in Supplemental Material [27]. When such a system is not

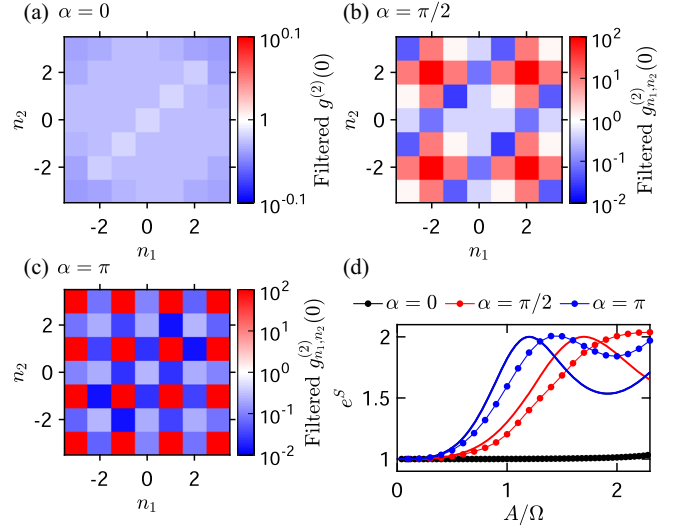


FIG. 2. Bichromatic photon-photon correlations. (a)–(c) Photon-photon correlations depending on the sideband numbers  $n_1$  and  $n_2$  calculated for  $A = 1.5 \Omega$ . Other parameters are  $\omega_0 d/c = 0$ ,  $\Omega = 200\gamma_{1D}$ ,  $\gamma_D = 5\gamma_{1D}$ . (d) Calculated exponential of the entanglement entropy  $e^S$  depending on the modulation strength  $A$  for resonant excitation,  $\varepsilon = \omega_0$ , and the relative modulation phase  $\alpha = 0, \pi/2, \pi$ . Thick lines show the analytical result derived in Supplemental Material [27].

perturbed by the modulation, the light couples only to the symmetric (even with respect to  $\mathcal{P}$ ) mode of the two qubits  $(\sigma_1^\dagger + \sigma_2^\dagger)|0\rangle$ , where  $\sigma_{1,2}^\dagger$  are the qubit raising operators. The parity symmetry also enforces strict constraints on the photon emission of the modulated system. If the qubit modulations are in phase,  $\alpha = 0$ , the photon can be scattered to any sideband. However, for  $\alpha = \pi$ , the qubit energy modulation is odd with respect to  $\mathcal{P}$ . The amplitude of the photon emitted into the sideband with an even (odd) number is an even (odd) function of  $A$ ; see Sec. 2G of the Supplemental Material for the rigorous proof [27]. Since it should be invariant under  $\mathcal{P}$ , only the even-order sidebands are present in the emission spectrum. Similarly, in the case of two-photon emission, all harmonics  $I_{n_1, n_2}^{(2)}$  are present if  $\alpha = 0$ , but for  $\alpha = \pi$  the  $\mathcal{P}$  symmetry dictates that the two-photon scattering process is allowed only if  $n_1 + n_2$  is even. These symmetry arguments indicate that the second-order cross-correlation function (3) should be very sensitive to the sideband numbers  $n_1$  and  $n_2$  when  $\alpha = \pi$ . In particular, for odd  $n_1, n_2$  we expect parity-protected photon bunching.

We have modeled the two-photon frequency-filtered photon detection scheme illustrated in Fig. 1 using the master equation formalism [35]; see Supplemental Material Sec. S3 for details [27]. Namely, the reflected photons are absorbed by the detectors D1 and D2 and the coincidence counts are calculated [36]. The detectors are modeled as two-level systems with the frequencies  $\omega_{D1} = \varepsilon + n_1\Omega$ ,  $\omega_{D2} = \varepsilon + n_2\Omega$ , and additional nonradiative decay with the rate  $\gamma_D$  that ensures that the detectors are always well below

the saturation. Figures 2(b)–2(d) present the calculated equal-time correlation function depending on the harmonic numbers  $n_1$  and  $n_2$  for three relative modulation phases  $\alpha = 0, \pi/2, \pi$ . In agreement with the symmetry analysis above, all the harmonics are present in the emission spectrum for symmetric modulation; see Fig. 2(b). When  $\alpha = \pi/2$ , Fig. 2(c), the two-photon correlation pattern becomes much richer and shows alternating photon bunching and anti-bunching depending on the values of  $n_1$  and  $n_2$ . This pattern is in qualitative agreement with our simplified theoretical model presented in Sec. S4 of the Supplemental Material. Finally, for antisymmetric modulation, presented in Fig. 2(d), the calculation reveals both parity-protected photon bunching, when  $n_1$  and  $n_2$  are odd, and parity-protected anti-bunching, when  $n_1$  and  $n_2$  have different parity.

*Entanglement of flying qudits.*—The emitted photons, residing in a superposition of the several frequency sidebands, can be regarded as many-level qudits. To quantify the two-qudit entanglement, we calculate the entanglement entropy [37,38]  $S = -\sum_\lambda |\lambda|^2 \ln |\lambda|^2$ , where  $\lambda$  is the singular value of the (normalized) two-photon wave function  $\psi_{n_1, n_2}$ . The latter is obtained numerically by calculating the correlation of the detectors D1 and D2 polarizations. The dependence of  $e^S$  on the modulation amplitude is shown in Fig. 2(d) for different relative modulation phases. For in-phase modulation,  $\alpha = 0$ , the entropy vanishes. That follows from the rigorous analytical expression for the scattering matrix of the homogeneously modulated system that differs from that of the system without modulation only by (time-dependent) phase factors; see Supplemental Material Sec. S2E [27]. For nonzero  $\alpha$ , the entropy increases with  $A$ , reaches the maximal value of  $\ln 2$ , and then oscillates below it. Thick lines in Fig. 2(d) show the analytical result neglecting the radiative coupling of the qubits (see Supplemental Material Sec. S5). It predicts that the modulation amplitude required to achieve  $S = \ln 2$  is given by  $A^* = j_0 \Omega / [2 \sin(\alpha/2)]$ , where  $j_0$  is the zero of the Bessel function  $J_0$ . Therefore, the antiphase modulation,  $\alpha = \pi$ , is favorable for maximal entanglement.

When  $S = \ln 2$ , photons are in a Bell state  $\psi_{n_1, n_2} = (u_{n_1} u_{n_2} + v_{n_1} v_{n_2}) / \sqrt{2}$ , where  $u_n$  and  $v_n$  are some orthogonal single-qudit states. Using single-qudit linear operations, that can be implemented by phase shapers and optical modulators [2], the Bell state can be converted to any other basis required for applications. Another approach is to consider nonharmonic modulation of the qubits, that enables us to generate any two-photon state described by a rank-2 matrix  $\psi_{n_1, n_2}$ , as described in Sec. S6 of the Supplemental Material [27].

Higher rank states can be generated with larger number of qubits  $N$ . As shown in Supplemental Material Sec. S7, the entanglement entropy of the state of  $M \geq 2$  photons emitted by  $N \geq M$  modulated qubits oscillates as a function of the modulation amplitude with several incommensurate periods and can reach the limiting value  $\ln N$  at certain

points. In particular, three qubits modulated with the amplitude  $A = j_0 \Omega / \sqrt{3}$  and the relative phases  $2\pi/3$  emit the three-photon state  $\psi_{n_1, n_2, n_3} = (u_{n_1} v_{n_2} w_{n_3} + \dots) / \sqrt{6}$ , where the ellipsis denotes the permutations of the indices, and  $u_n, v_n,$  and  $w_n$  are three orthogonal states. Such a state possesses the maximally possible entanglement entropy of  $\ln 3$  and is an analog of the cluster state: indeed, if one of the photons is measured (in the  $u, v, w$  basis), the two other photons remain in the entangled Bell state. Similar states of four and more photons can also be generated. While the cluster states could be very important for many quantum computing applications, it is yet unclear how wide the class of many-photon states that can be generated by the proposed scheme is, e.g., if more complex matrix product states are feasible.

*Time-dependent correlations.*—Signatures of the sideband cross-correlations can be observed even without frequency filtering in the time dependence of the total second-order correlation function,

$$g^{(2)}(t + \tau, t) = \frac{\langle a^\dagger(t + \tau) a^\dagger(t) a(t) a(t + \tau) \rangle}{[\langle a^\dagger a \rangle_0]^2}, \quad (4)$$

where  $a$  is the annihilation operator corresponding to the reflected photons, and  $\langle \dots \rangle$  and  $\langle \dots \rangle_0$  denote averaging over the state of the system with and without modulation, respectively. Because of the temporal modulation of the qubit resonance frequencies, the correlation function  $g^{(2)}$  is no longer a function of delay time  $\tau$  only, but also depends on the absolute time  $t$  [39] with the period  $2\pi/\Omega$ . This allows us to present the correlation function as the Fourier series  $g^{(2)}(t + \tau, t) = \sum_{n=-\infty}^{\infty} e^{-in\Omega t} g_n^{(2)}(\tau)$ . We will focus on the harmonics  $g_n^{(2)}(\tau)$  at zero delay  $\tau = 0$ .

The numerator of the total correlation function Eq. (4) is determined by the squared sum,

$$\langle a^\dagger(t + \tau) a^\dagger(t) a(t) a(t + \tau) \rangle = \left| \sum_n S_n(\tau) e^{-i\Omega t} \right|^2, \quad (5)$$

where  $S_n$  is the amplitude of the two-photon scattering process, characterized by photon pair energy change  $2\varepsilon \rightarrow 2\varepsilon + n\Omega$ . A general approach for few-photon scattering in Floquet systems was developed in Ref. [40]. Here we use a similar perturbative diagrammatic approach to calculate  $S_n$  (see Supplemental Material Sec. S2 [27]). Using Eqs. (4) and (5), we obtain the expression for the  $n$ th harmonic of the total two-photon correlation function,  $g_n^{(2)}(\tau) \propto \sum_{k=-\infty}^{\infty} S_{n+k}(\tau) S_k^*(\tau)$ . In particular, for low modulation amplitude  $A$  we have  $S_n \propto A^{|n|}$ , so the  $n = \pm 1$  harmonic  $g_1^{(2)} \propto A$  is governed by  $S_1 S_0^* + S_0 S_{-1}^*$ . Here  $S_{\pm 1}$  correspond to amplitudes of the first-order anti-Stokes and Stokes two-photon scattering processes  $2\varepsilon \rightarrow 2\varepsilon \pm \Omega$ . In the considered resolved-sideband regime,

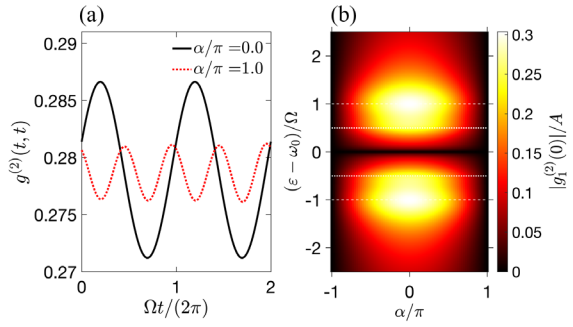


FIG. 3. (a) Time-dependent photon-photon correlations  $g^{(2)}(t, \tau = 0)$  calculated for  $\varepsilon - \omega_0 = \Omega$ . Black solid and red dotted curves correspond to in-phase ( $\alpha = 0$ ) and out-of-phase ( $\alpha = \pi$ ) modulation of the first and second qubit resonance frequencies. (b) Color map of the correlation function first temporal harmonic  $|g_1^{(2)}(0)|$  as a function of relative modulation phase  $\alpha$  and frequency detuning of the incident light  $\varepsilon - \omega$ . The calculation parameters are  $\Omega = 5\gamma_{1D}$ ,  $A = 0.025\gamma_{1D}$ .

they are determined by the probability of the two-photon scattering into the sidebands with energies  $\varepsilon$  and  $\varepsilon \pm \Omega$ :  $I_{0,\pm 1}^{(2)} \propto |S_{\pm 1}(0)|^2$ .

Our consideration of frequency-filtered correlations above has demonstrated that for antisymmetric modulation  $\alpha = \pi$ , one has  $I_{\pm 1,0}^{(2)} \propto |S_{\pm 1}(0)|^2 \rightarrow 0$ . Thus, we expect that for such modulation the  $n = \pm 1$  harmonic  $g_1^{(2)}$  will be absent in the Fourier series. This is confirmed by the rigorous calculation of the total time-dependent zero-delay correlation function  $g^{(2)}(t, t)$ , shown in Fig. 3(a). Black solid and red dotted curves correspond to  $\alpha = 0$  and  $\alpha = \pi$ , respectively. It is clearly seen from the calculation that for  $\alpha = \pi$  the period of the dependence is twice smaller than that for  $\alpha = 0$ . This indicates the absence of the first harmonic  $\propto e^{\mp i\Omega t}$  in the former case and provides a direct manifestation of the parity-protected antibunching in the time-dependent photon-photon correlations.

Figure 3(b) examines the dependence of the time-resolved correlations on the relative modulation phase  $\alpha$  and the incident frequency detuning  $\varepsilon - \omega$  in more detail. The color shows the numerically calculated amplitude of the first harmonic  $|g_1^{(2)}(0)|/A$  (at  $A \rightarrow 0$ ). In agreement with the results in Figs. 2 and 3(a), the correlations are suppressed if  $\alpha = \pm\pi$  for any incident light frequency  $\varepsilon$ . The strongest correlations are achieved for the in-phase modulation,  $\alpha = 0$ . The calculation also shows suppression of the harmonic  $g_1^{(2)}(0)$  for resonant pumping, when  $\varepsilon = \omega_0$ . Even though the intensities of the Stokes and anti-Stokes two-photon scattering processes are nonzero in that case,  $I_{0,\pm 1}^{(2)} \propto |S_{\pm 1}(0)|^2 \neq 0$ , as was illustrated in Fig. 2, the interference of the two contributions to  $g_1^{(2)}(0)$  stemming from the Stokes and anti-Stokes processes turns out to be destructive,  $S_1(0)S_0^*(0) + S_0(0)S_{-1}^*(0) = 0$  at  $\varepsilon = \omega_0$ .

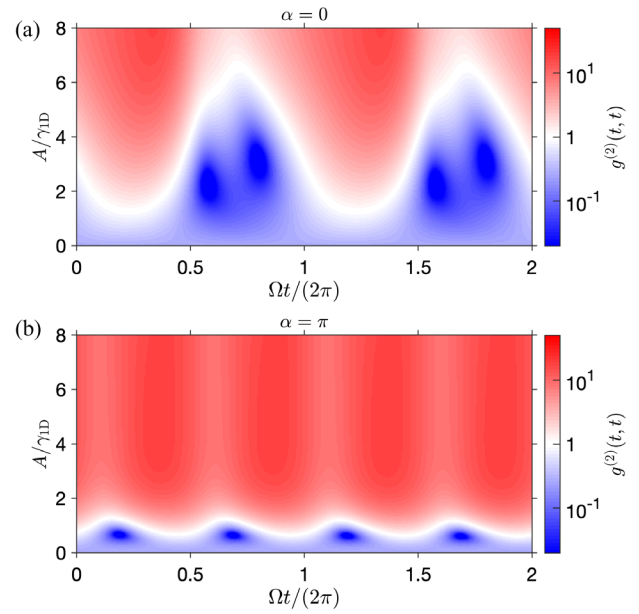


FIG. 4. Total time-dependent photon-photon correlation function  $g^{(2)}(t, t)$  depending on the modulation amplitude for (a) in-phase and (b) out-of-phase modulation of the first and second qubit resonance frequencies. Calculation was performed for  $\varepsilon = \omega_0 + \Omega$ ,  $\Omega = 5\gamma_{1D}$ .

Note that  $g_1^{(2)}(\tau)$  in this case is still nonzero if a finite delay time  $\tau \neq 0$  is considered.

As a function of pump frequency, the  $g_1^{(2)}$  harmonic has two pairs of Stokes or anti-Stokes resonances: stronger single-photon resonances at  $\varepsilon = \omega_0 \pm \Omega$  and weaker two-photon resonances at  $2\varepsilon = 2\omega_0 \pm \Omega$ , marked by dashed and dotted lines in Fig. 3(b), respectively. At these resonances, the first harmonic of the correlation function reads

$$\begin{aligned} g_1^{(2)}(0) &= \pm \frac{iA}{4\gamma_{1D}} \cos \frac{\alpha}{2}, & \varepsilon = \omega_0 \pm \Omega, \\ g_1^{(2)}(0) &= \pm \frac{7A}{6\Omega} \cos \frac{\alpha}{2}, & \varepsilon = \omega_0 \pm \frac{\Omega}{2}, \end{aligned} \quad (6)$$

where we supposed  $\Omega \gg \gamma_{1D}$ ; see also Sec. S3 of the Supplemental Material [27] for more general analytical expressions.

*Strong modulation.*—Up to now we focused on the weak modulation case, when only the first-order Stokes and anti-Stokes scattering is considerable. For strong modulation additional sidebands emerge, leading to high-order harmonics  $g_n^{(2)}$  in the temporal dependence of the total correlation function. Figure 4 shows the dependence of  $g^{(2)}(t, t)$  on  $A$  for (a) symmetric and (b) antisymmetric modulation. Similarly to the case of small  $A$  [Fig. 3(a)], the temporal period for antiphase modulation is twice smaller than that for the in-phase modulation. This indicates the absence of all odd-order harmonics for  $\alpha = \pi$ , in agreement

with the parity argument forbidding two-photon scattering processes  $2\varepsilon \rightarrow 2\varepsilon + (2k+1)\Omega$ . Then, substituting  $S_{2k+1} = 0$  into  $g_n^{(2)}(\tau)$ , we indeed conclude that  $g_{2k+1}^{(2)} = 0$ .

The correlations change significantly with the modulation strength. For low  $A$ , a relatively weak overall antibunching is observed for both in-phase and antiphase modulation. With increase of  $A$ , the antibunching first becomes stronger, reaching maximum for  $A/\gamma_{1D} \approx 3$  (0.7), then a bunching appears during certain time intervals, and finally the antibunching gets completely replaced by a pronounced bunching at  $A/\gamma_{1D} \gtrsim 6$  (1.2) for the case of (anti)symmetric modulation. This behavior for  $\alpha = 0$  is well explained by Eq. (6) that suggests that the amplitude  $|g_1^{(2)}|$  increases linearly with  $A$  and should reach the value of the order of unity at the threshold  $A \sim \gamma_{1D}$ . Then, it can overcome the constant contribution  $g_0^{(2)}$ , enabling the change of the  $g^{(2)}(t, t)$  sign. Similarly, for  $\alpha = \pi$  when  $g_1^{(2)} = 0$ , the second harmonic  $g_2^{(2)}$  grows with  $A$  and reaches unity at  $A \sim \gamma_{1D}$ .

*Summary.*—We have considered theoretically a waveguide QED setup where the qubit resonance frequencies are modulated periodically in time. We predict that by tuning the relative phase of modulation for different qubits, one can realize multiphoton frequency comb in qubit emission with controllable correlations of photons at different frequencies which could be very useful in the modern optical quantum computing experiments. Our results open the way for deterministic generation and processing of entangled multiphoton states in systems with high cooperativities, such as optical chips or chips based on superconducting qubits.

We are grateful to E. S. Redchenko for useful discussions. The study of two-photon correlations was funded by the Russian Science Foundation Project No. 20-12-00194. The work of A. V. P. was supported by Rosatom in the framework of the Roadmap for Quantum computing (Contract No. 868-1.3-15/15-2021 and Contract No. R2152). A. V. P. also acknowledges support from the Grant No. MK-4191.2021.1.2 and the Foundation “Basis”. The density matrix evolution simulation was conducted with the support of Russian Science Foundation Project No. 20-12-00224. I. V. I. acknowledges the support of RFBR-DFG Project No. 21-52-12038, “BASIS” foundation and ITMO Priority 2030 program.

\*alexander.poddubnyy@weizmann.ac.il

†i.iorsh@metalab.ifmo.ru

- [1] Michael Kues, Christian Reimer, Joseph M. Lukens, William J. Munro, Andrew M. Weiner, David J. Moss, and Roberto Morandotti, Quantum optical microcombs, *Nat. Photonics* **13**, 170 (2019).  
 [2] Hsuan-Hao Lu, Joseph M. Lukens, Nicholas A. Peters, Ogaga D. Odele, Daniel E. Leaird, Andrew M. Weiner, and

- Pavel Lougovski, Electro-optic Frequency Beam Splitters and Tritters for High-Fidelity Photonic Quantum Information Processing, *Phys. Rev. Lett.* **120**, 030502 (2018).  
 [3] Joseph M. Lukens and Pavel Lougovski, Frequency-encoded photonic qubits for scalable quantum information processing, *Optica* **4**, 8 (2017).  
 [4] T. C. Ralph, I. Söllner, S. Mahmoodian, A. G. White, and P. Lodahl, Photon Sorting, Efficient Bell Measurements, and a Deterministic Controlled- $z$  Gate Using a Passive Two-Level Nonlinearity, *Phys. Rev. Lett.* **114**, 173603 (2015).  
 [5] Netanel H. Lindner and Terry Rudolph, Proposal for Pulsed On-Demand Sources of Photonic Cluster State Strings, *Phys. Rev. Lett.* **103**, 113602 (2009).  
 [6] Hannes Pichler, Soonwon Choi, Peter Zoller, and Mikhail D. Lukin, Universal photonic quantum computation via time-delayed feedback, *Proc. Natl. Acad. Sci. U.S.A.* **114**, 11362 (2017).  
 [7] Ivan Marcikic, Hugues De Riedmatten, Wolfgang Tittel, Hugo Zbinden, and Nicolas Gisin, Long-distance teleportation of qubits at telecommunication wavelengths, *Nature (London)* **421**, 509 (2003).  
 [8] Nicolas Gisin, Grégoire Ribordy, Wolfgang Tittel, and Hugo Zbinden, Quantum cryptography, *Rev. Mod. Phys.* **74**, 145 (2002).  
 [9] C. Monroe, R. Raussendorf, A. Ruthven, K. R. Brown, P. Maunz, L.-M. Duan, and J. Kim, Large-scale modular quantum-computer architecture with atomic memory and photonic interconnects, *Phys. Rev. A* **89**, 022317 (2014).  
 [10] C. T. Nguyen, D. D. Sukachev, M. K. Bhaskar, B. Machielse, D. S. Levonian, E. N. Knall, P. Stroganov, R. Riedinger, H. Park, M. Lončar *et al.*, Quantum Network Nodes Based on Diamond Qubits with an Efficient Nanophotonic Interface, *Phys. Rev. Lett.* **123**, 183602 (2019).  
 [11] P.-O. Guimond, B. Vermersch, M. L. Juan, A. Sharafiev, G. Kirchmair, and P. Zoller, A unidirectional on-chip photonic interface for superconducting circuits, *npj Quantum Inf.* **6**, 32 (2020).  
 [12] Alexandra S. Sheremet, Mihail I. Petrov, Ivan V. Iorsh, Alexander V. Poshakinskiy, and Alexander N. Poddubny, Waveguide quantum electrodynamics: Collective radiance and photon-photon correlations, [arXiv:2103.06824](https://arxiv.org/abs/2103.06824).  
 [13] Jung-Tsung Shen and Shanhui Fan, Strongly Correlated Two-Photon Transport in a One-Dimensional Waveguide Coupled to a Two-Level System, *Phys. Rev. Lett.* **98**, 153003 (2007).  
 [14] Adarsh S. Prasad, Jakob Hinney, Sahand Mahmoodian, Klemens Hammerer, Samuel Rind, Philipp Schneeweiss, Anders S. Sørensen, Jürgen Volz, and Arno Rauschenbeutel, Correlating photons using the collective nonlinear response of atoms weakly coupled to an optical mode, *Nat. Photonics* **14**, 719 (2020).  
 [15] Iacopo Carusotto, Andrew A. Houck, Alicia J. Kollár, Pedram Roushan, David I. Schuster, and Jonathan Simon, Photonic materials in circuit quantum electrodynamics, *Nat. Phys.* **16**, 268 (2020).  
 [16] Bharath Kannan, Daniel L. Campbell, Francisca Vasconcelos, Roni Winik, D. K. Kim, Morten Kjaergaard, Philip Krantz, Alexander Melville, Bethany M. Niedzielski, J. L. Yoder *et al.*, Generating spatially entangled itinerant

- photons with waveguide quantum electrodynamics, *Sci. Adv.* **6**, eabb8780 (2020).
- [17] Srivatsan Chakram, Kevin He, Akash V. Dixit, Andrew E. Oriani, Ravi K. Naik, Nelson Leung, Hyeokshin Kwon, Wen-Long Ma, Liang Jiang, and David I. Schuster, Multimode photon blockade, *Nat. Phys.* **18**, 879 (2022).
- [18] Christof Weitenberg and Juliette Simonet, Tailoring quantum gases by Floquet engineering, *Nat. Phys.* **17**, 1342 (2021).
- [19] Huiyao Y. Chen, E. R. MacQuarrie, and Gregory David Fuchs, Orbital State Manipulation of a Diamond Nitrogen-Vacancy Center Using a Mechanical Resonator, *Phys. Rev. Lett.* **120**, 167401 (2018).
- [20] Kevin C. Miao, Alexandre Bourassa, Christopher P. Anderson, Samuel J. Whiteley, Alexander L. Crook, Sam L. Bayliss, Gary Wolfowicz, Gergő Thiering, Péter Udvarhelyi, Viktor Ivády *et al.*, Electrically driven optical interferometry with spins in silicon carbide, *Sci. Adv.* **5**, aay0527 (2019).
- [21] Daniil M. Lukin, Alexander D. White, Rahul Trivedi, Melissa A. Guidry, Naoya Morioka, Charles Babin, Öney O. Soykal, Jawad Ul-Hassan, Nguyen Tien Son, Takeshi Ohshima *et al.*, Spectrally reconfigurable quantum emitters enabled by optimized fast modulation, *npj Quantum Inf.* **6**, 80 (2020).
- [22] Kevin G. Schädler, Carlotta Ciancico, Sofia Pazzagli, Pietro Lombardi, Adrian Bachtold, Costanza Toninelli, Antoine Reserbat-Plantey, and Frank H. L. Koppens, Electrical control of lifetime-limited quantum emitters using 2D materials, *Nano Lett.* **19**, 3789 (2019).
- [23] Elena S. Redchenko, Alexander V. Poshakinskiy, Riya Sett, Martin Zemlicka, Alexander N. Poddubny, and Johannes M. Fink, Tunable directional photon scattering from a pair of superconducting qubits, [arXiv:2205.03293](https://arxiv.org/abs/2205.03293).
- [24] Qian Bin, Xin-You Lü, Fabrice P. Laussy, Franco Nori, and Ying Wu,  $n$ -Phonon Bundle Emission via the Stokes Process, *Phys. Rev. Lett.* **124**, 053601 (2020).
- [25] M. K. Schmidt, R. Esteban, G. Giedke, J. Aizpurua, and A. González-Tudela, Frequency-resolved photon correlations in cavity optomechanics, *Quantum Sci. Technol.* **6**, 034005 (2021).
- [26] Chao-Yuan Jin, Robert Johne, Milo Y. Swinkels, Thang B. Hoang, Leonardo Midolo, Peter J. Van Veldhoven, and Andrea Fiore, Ultrafast non-local control of spontaneous emission, *Nat. Nanotechnol.* **9**, 886 (2014).
- [27] See Supplemental Material at <http://link.aps.org/supplemental/10.1103/PhysRevLett.130.023601> for a detailed description of the model, description of the diagrammatic technique, details of the density matrix calculations, derivation of the selection rules for the photon-photon correlations, and a detailed description of the protocol to generate entangled states, which includes Refs. [28–33].
- [28] J. Dalibard and S. Reynaud, Correlation signals in resonance fluorescence: Interpretation via photon scattering amplitudes, *J. Phys. (Les Ulis, Fr.)* **44**, 1337 (1983).
- [29] A. V. Poshakinskiy and A. N. Poddubny, Biexciton-mediated superradiant photon blockade, *Phys. Rev. A* **93**, 033856 (2016).
- [30] T. Caneva, M. T. Manzoni, T. Shi, J. S. Douglas, J. I. Cirac, and D. E. Chang, Quantum dynamics of propagating photons with strong interactions: A generalized input–output formalism, *New J. Phys.* **17**, 113001 (2015).
- [31] Y. Ke, A. V. Poshakinskiy, C. Lee, Y. S. Kivshar, and A. N. Poddubny, Inelastic Scattering of Photon Pairs in Qubit Arrays with Subradiant States, *Phys. Rev. Lett.* **123**, 253601 (2019).
- [32] H. Carmichael, *An Open Systems Approach to Quantum Optics* (Springer, New York, 1993).
- [33] P. Migdał, J. Rodriguez-Laguna, and M. Lewenstein, Entanglement classes of permutation-symmetric qudit states: Symmetric operations suffice, *Phys. Rev. A* **88**, 012335 (2013).
- [34] Francesco Pagliano, YongJin Cho, Tian Xia, Frank Van Otten, Robert Johne, and Andrea Fiore, Dynamically controlling the emission of single excitons in photonic crystal cavities, *Nat. Commun.* **5**, 5786 (2014).
- [35] Kevin Lalumière, Barry C. Sanders, A. F. van Loo, A. Fedorov, A. Wallraff, and A. Blais, Input-output theory for waveguide QED with an ensemble of inhomogeneous atoms, *Phys. Rev. A* **88**, 043806 (2013).
- [36] E. del Valle, A. Gonzalez-Tudela, F. P. Laussy, C. Tejedor, and M. J. Hartmann, Theory of Frequency-Filtered and Time-Resolved  $n$ -Photon Correlations, *Phys. Rev. Lett.* **109**, 183601 (2012).
- [37] J. Eisert, M. Cramer, and M. B. Plenio, Colloquium: Area laws for the entanglement entropy, *Rev. Mod. Phys.* **82**, 277 (2010).
- [38] Alexander V. Poshakinskiy and Alexander N. Poddubny, Dimerization of Many-Body Subradiant States in Waveguide Quantum Electrodynamics, *Phys. Rev. Lett.* **127**, 173601 (2021).
- [39] A. V. Poshakinskiy and S. A. Tarasenko, Spin noise at electron paramagnetic resonance, *Phys. Rev. B* **101**, 075403 (2020).
- [40] Rahul Trivedi, Alex White, Shanhui Fan, and Jelena Vučković, Analytic and geometric properties of scattering from periodically modulated quantum-optical systems, *Phys. Rev. A* **102**, 033707 (2020).